Journal Pre-proof

Evaluation of human umbilical vein endothelial cells growth onto heparin-modified electrospun vascular grafts

Pablo C. Caracciolo, Patricia Diaz-Rodriguez, Inés Ardao, David Moreira, Florencia Montini-Ballarin, Gustavo A. Abraham, Angel Concheiro, Carmen Alvarez-Lorenzo

PII: S0141-8130(21)00525-0

DOI: https://doi.org/10.1016/j.ijbiomac.2021.03.008

Reference: BIOMAC 18054

To appear in: *International Journal of Biological Macromolecules*

Received date: 25 October 2020

Revised date: 26 February 2021

Accepted date: 2 March 2021

Please cite this article as: P.C. Caracciolo, P. Diaz-Rodriguez, I. Ardao, et al., Evaluation of human umbilical vein endothelial cells growth onto heparin-modified electrospun vascular grafts, *International Journal of Biological Macromolecules* (2018), https://doi.org/10.1016/j.ijbiomac.2021.03.008

This is a PDF file of an article that has undergone enhancements after acceptance, such as the addition of a cover page and metadata, and formatting for readability, but it is not yet the definitive version of record. This version will undergo additional copyediting, typesetting and review before it is published in its final form, but we are providing this version to give early visibility of the article. Please note that, during the production process, errors may be discovered which could affect the content, and all legal disclaimers that apply to the journal pertain.

© 2018 Published by Elsevier.

Journal Pre-proof

Evaluation of human umbilical vein endothelial cells growth onto heparin-modified electrospun vascular grafts

Pablo C. Caracciolo[1]*[#], Patricia Diaz-Rodriguez[2#], Inés Ardao[3], David Moreira[3], Florencia Montini-Ballarin[1], Gustavo A. Abraham[1], Angel Concheiro[2], Carmen Alvarez-Lorenzo[2]

[1]Instituto de Investigaciones en Ciencia y Tecnología de Materiales, INTEMA (UNMdP-CONICET), Av. Cristóbal Colón 10850, B7606WV, Mar del Plata, Argentina

[2]Departamento de Farmacología, Farmacia y Tecnología Farmacéutica, I+D Farma (GI-1645), Facultad de Farmacia and Health Research Institute of Santiago de Compostela (IDIS), Universidade de Santiago de Compostela, 15782-Santiago de Compostela, Spain

[3]BioFarma Research group, Center for Research in Molecular Medicine and Chronic Diseases (CiMUS), Universidade de Santiago de Compostela, 15782 Santiago de Compostela, Spain

[#]Both authors contributed equally to this work.

*Correspondence should be addressed to:
Pablo C. Caracciolo
pcaracciolo@fi.mdp.edu.ar
INTEMA (UNMdP-CONICET)
Phone number: +54 223 6260630
Address: Av. Cristóbal Colón 10850
Zip code: B7606WV
Mar del Plata, Argentina

Journal Pre-proof

Abstract

One of the main challenges of cardiovascular tissue engineering is the development of bioresorbable and compliant small-diameter vascular grafts (SDVG) for patients where autologous grafts are not an option. In this work, electrospun bilayered bioresorbable SDVG based on blends of poly(L-lactic acid) (PLLA) and segmented polyurethane (PHD) were prepared and evaluated. The inner layer of these SDVG was surface-modified with heparin, following a methodology involving PHD urethane functional groups. Heparin was selected as anticoagulant agent, and also due to its ability to promote human umbilical vein endothelial cells (HUVECs) growth and to inhibit smooth muscle cells over-proliferation, main cause of neointimal hyperplasia and restenosis. Immobilized heparin was quantified and changes in SDVG microstructure were investigated through SEM. Tensile properties of the heparin-functionalized SDVG resembled those of saphenous vein. Vascular grafts were seeded with HUVECs and cultured on a flow-perfusion bioreactor to analyze the effect of heparin on graft endothelization under simulated physiological-like conditions. The analysis of endothelial cells attachment and gene expression (Real-Time PCR) pointed out that the surface functionalization with heparin successfully promoted a stable and functional endothelial cell layer.

Keywords: bioresorbable vascular grafts; surface modification; heparin; human umbilical vein endothelial cells (HUVECs); biological characterization

Journal Pre-proof

Abbreviations:

DAPEG: poly(ethylene glycol) bis(amine)

EDC: 1-(3-dimethylaminopropyl)-3-ethylcarbodiimide hydrochloride

HUVECs: human umbilical vein endothelial cells

NaOCl: sodium hypochlorite

PBS: phosphate buffer saline

PEG: poly(ethylene glycol)

PHD: PCL-based segmented polyurethane

PLLA: poly (L-lactic acid)

SDVG: small-diameter vascular grafts

sNHS: *N*-hydroxysulfosuccinimide sodium salt

SPU: segmented polyurethane

TFE: 2,2,2-trifluoroethanol

Journal Pre-proof

1. Introduction

Cardiovascular diseases are one of the leading causes of death worldwide. Coronary and peripheral arteries disorders are among the most common cardiovascular affections [1,2]. When less invasive alternatives fail, the classic treatment is bypass surgery, employing large saphenous vein (LSV) or internal thoracic artery as gold standard grafts. However, their use is limited by the donors' availability (allograft) and individual anatomical features (autograft). The allograft approach can lead to rejection, and thus, to the failure of the therapy [3]. On the other hand, autograft involves the morbidity of a double surgical intervention, and more than 40% of patients do not have proper autologous grafts [4]. In addition, for the case of aortocoronary and femoral-popliteal bypass, the patency rates of arterial LSV grafting are far from ideal [5]. Depending on the affection, stents appear as an alternative solution to overcome these problems, but usually fail in the long term mainly due to hyperplasia and restenosis. Synthetic vascular grafts, such as those obtained from Dacron® (PET, poly(ethylene terephthalate)) and Goretex® (ePTFE, expanded poly(tetrafluoro ethylene)), have been employed since the 50's and 60's, respectively. These grafts display a good performance as replacement for large arteries [6,7], but they present higher stiffness than required for small-diameter vascular grafts (SDVG, < 6 mm), low endothelialization rate and may trigger acute thrombosis, intimal hyperplasia, stenosis, and calcification [8-13]. Thus, the ideal SDVG with adequate surface quality, namely non-thrombogenic and good endothelialization rate, and biomechanical behavior has yet to be produced.

Electrospinning is a versatile technology to obtain nanofibrous scaffolds that mimic the extracellular matrix structure of native tissues and provide an adequate microenvironment for cell adhesion and proliferation [14-17]. In previous works we prepared bilayered tubular electrospun scaffolds from two materials possessing complementary features to mimic the mechanical behavior of veins and arteries [18]; namely, high compliance at low pressure ranges, and high elastic modulus to withstand high stress requirements at high pressures [19,20]. Thus, synthesized aliphatic bioresorbable segmented poly(ester urethane) (SPU) PHD [21,22] providing an elastin-like behavior, and FDA-approved bioresorbable poly (L-lactic acid) (PLLA) exhibiting high elastic modulus and mechanical performance similar to that of collagen were employed [23]. Based on the collagen/elastin ratio of muscular arteries [24,25], PLLA/PHD 50/50 and 90/10 blend ratios were selected as the SDVG inner and outer layers to mimic native "media" and "adventitia", respectively [23].

Although adequate mechanical behavior is crucial for the success of vascular devices [13,26], surface properties are also critical. Surface modification of SDVG by covalent bonding of different molecules has been widely explored, mainly to improve hemocompatibility, cell adhesion and proliferation [27,28] and, what is crucial for small-diameter blood vessels, to

prevent thrombogenic events [29-32]. Heparin has been extensively used in vascular therapy as anticoagulant agent and can also inhibit the over-proliferation of smooth muscle cells, which is the main reason for neointimal hyperplasia and restenosis [33]. Moreover, it can promote endothelial cells growth [34]. For these reasons, heparin was selected in a previous experiment to explore two different surface modification techniques from flat surfaces of PLLA/PHD 50/50 electrospun matrices, prepared with same composition as the inner layer of the previously designed SDVG [35]. A PEG spacer was employed since heparin bioactivity usually decreases when directly grafted onto biomaterials surface, as its mobility is reduced [36]. Heparin functionalization from PHD urethane groups has been shown to be more efficient (higher grafting density) than PLLA ester hydrolysis and functionalization, and also inhibited platelet adhesion to higher extent. These previous results suggested that the adequate modification of only one polymer present at the blend scaffold could be enough to minimize the risk of *in vivo* platelet attachment. In addition, the fact that no chain scission is involved in the urethane methodology is advantageous to ensure other properties keep unchanged.

In the present work we aim to move forward and perform heparin immobilization through urethane methodology of PLLA/PHD electrospun vascular grafts. Functionalized SDVG were *in vitro* characterized in terms of heparin immobilization, tensile properties and biological performance. SDVG were seeded with endothelial cells and cultured on a flow perfusion bioreactor to evaluate graft endothelization under physiological-like conditions. The cell attachment quantification clearly pointed out the beneficial effect of heparin on endothelial cell adhesion and spreading. Moreover, the HUVECs gene expression analysis indicated that endothelial cells seeded on functionalized grafts increased the expression of von Willebrand Factor, which is key in controlling the hemostatic process, indicating the formation of a functional endothelial cell layer.

2. Materials and methods

2.1. Materials

PLLA (PLA2002D Mn = 78.02 kg mol^{-1}, Mw = 129.91 kg mol^{-1}, IP = 1.67) was obtained from NatureWorks L.L.C. (MN, USA). 2,2,2-Trifluoroethanol (TFE) and poly(ethylene glycol) bis(amine) (DAPEG, Mn ≈ 3.4 kg mol^{-1}) were acquired from Sigma-Aldrich (St. Louis, MO, USA). Disodium hydrogen phosphate (Na_2HPO_4) and sodium dihydrogen phosphate (NaH_2PO_4) were purchased from Merck (Germany). 2-(4-Morpholino)ethanesulfonic acid (MES) was obtained from Fisher Scientific (UK). 1-(3-Dimethylaminopropyl)-3-ethylcarbodiimide hydrochloride (EDC, +98%), *N*-hydroxysulfosuccinimide sodium salt (sNHS, 95%), sodium hypochlorite (NaOCl), sodium

hydrosulfite ($Na_2S_2O_4$), and allyl glycidyl ether ($C_6H_{10}O_2$, +99%) were purchased from Acros Organics (NJ, USA). Heparin sodium salt from porcine intestinal mucosa (Mn ≈ 15 kg mol^{-1}, 192 U mg^{-1}) was obtained from Calbiochem®, EMD Millipore Corp. (MA, USA). Sodium chloride (NaCl) was obtained from Analar NORMAPUR, Prolabo®, VWR International (Belgium). Toluidine blue was obtained from Panreac (Spain). Solvents and reagents were used as received.

2.2. Synthesis of segmented poly(ester urethane)

SPU, named PHD, was synthesized from aliphatic diisocyanate (HDI), aliphatic polyester (poly(ε-caprolactone) diol, PCL diol), and a novel aromatic chain extender according to previously reported procedures [21]. Intrinsic viscosity [η] was measured using an Ubbelohde Type OC viscosimeter (Canon, Japan) and *N*,*N*-dimethylacetamide (DMAc) as solvent at 30 ± 0.1ºC. The number average (Mn) and the weight average molecular weight (Mw) were determined by gel permeation chromatography (GPC, Waters, Special Solvents (DMA) Empower Software) in DMAc with LiBr (0.42 g/mL) at 35ºC.

2.3. Preparation of electrospun SDVG

A standard electrospinning setup was used, consisting of a programmable syringe pump (Activa A22 ADOX S.A., Argentina), a high-voltage power source (ES30P, Gamma High Voltage Research Inc., USA), and a 5 mm-diameter rototranslating mandrel as collector. Each of the as-prepared solutions was loaded into a standard 10 mL plastic syringe connected to a poly(tetrafluoro ethylene) tube, attaching to the open end a blunt 18-gauge stainless steel needle as a nozzle. All experiments were carried out at 23ºC in a chamber with a ventilation system.

Bilayered vascular grafts were produced by sequential electrospinning, with the inner layer on the lumen side (PLLA/PHD 50/50 wt/wt) and the outer layer on the external side (PLLA/PHD 90/10 wt/wt). A total concentration of 23% wt/v in TFE was used for the inner layer and 20% wt/v in TFE for the outer layer. The electrospinning parameters were set according to previously reported conditions [18]. Briefly, a mandrel rotation speed of 1000 rpm and a distance to collector of 15 cm were used for both layers, while applied voltages of 13 kV and 15 kV, translational speeds of 2 mm/s and 1 mm/s, and flow rates of 1 ml/h and 0.5 ml/h, were used for the inner and outer layers, respectively. The internal diameter was approximately of 5 mm.

The electrospun scaffolds were dried under vacuum at room temperature to remove residual solvent, and finally stored in a desiccator.

2.4. Surface modification of PLLA/PHD electrospun SDVG

The surface modification was carried out by urethane functionalization as previously reported [35]. First, scaffolds were modified by activating urethane functional groups through stirring in orbital shaker at 60 rpm with a 0.15 mol/L PBS (pH 6.0) buffer solution containing 0.3% wt/wt NaOCl for 25 min. Then, they were washed thrice with 0.15 mol/L PBS pH 6 solution for 10 min, and thrice with a 0.15 mol/L PBS (pH 8.0) buffer solution. After that, scaffolds were incubated with a 0.15 mol/L PBS (pH 8.0) buffer solution containing 0.1% wt/wt $Na_2S_2O_4$ as initiator and 5% wt/wt allyl glycidyl ether as a monomer for 48 h and washed 10 times with the buffer solution [37]. Then, they were treated with PBS (pH 8.0) buffer solution containing 1.33 mg/mL DAPEG for 60 h at 40ºC. The resulting scaffolds were first washed with a 0.1 mol/L Na_2HPO_4 solution for 1 h, a 2 mol/L NaCl solution for 2 h to fully eliminate the unreacted DAPEG, five times with a 0.1 mol/L PBS (pH 7.0) buffer solution, and treated with a heparin solution prepared as follows: a 0.05 mol/L MES (pH 5.6) buffer solution containing 5 mg/mL heparin, 0.65 mg/mL EDC and 0.72 mg/mL sNHS was incubated for 30 min at room temperature in orbital shaker and then mixed in a 1:1 ratio with a 0.25 mol/L PBS (pH 7.2) buffer solution immediately before functionalization, to achieve a final pH 7.0 [38]. Finally, scaffolds were incubated for 6 h at room temperature in orbital shaker at 60 rpm, washed with a 0.1 mol/L Na_2HPO_4 solution for 1 h, twice with a 2 mol/L NaCl solution for 1 h, and five times with a 0.1 mol/L PBS (pH 7.0) buffer solution and dried under vacuum at room temperature.

2.5. Characterization

2.5.1. Quantification of immobilized heparin

The amount of heparin bound to the surface of the scaffolds was determined by the toluidine blue staining method. First, standard heparin solutions ranging from 0 to 250 µg/mL were prepared in 8 x 10^{-4}% (wt/v) toluidine blue aqueous solution to obtain a standard curve. After shaking in an orbital shaker at 220 rpm for 1 h, 2 mL of these solutions were added to 3 mL of n-hexane. The resulting mixtures were shaken again at 220 rpm for 30 min, so that the toluidine blue-heparin complex was extracted into the organic layer. The calibration curve was built from the remaining aqueous solutions. Then, 0.64 cm^2-discs cut from samples with and without immobilized heparin were placed in toluidine blue aqueous solution, and the same procedure was performed. Finally, absorbance of the remaining toluidine blue in the aqueous phase was measured at 631 nm in an UV-Vis spectrophotometer (Agilent 8453, Agilent Technologies, Germany). The concentration of immobilized heparin on the scaffolds was determined from the standard curve [39,40].

2.5.2. SEM analysis

SEM micrographs of the electrospun scaffolds before and after heparin functionalization were recorded in a Zeiss FESEM Ultra Plus equipment after coating with iridium. Samples were cut longitudinally with a scalpel, and the external and internal surfaces were observed. The diameter of at least 100 fibers was measured and averaged for each sample (Image Pro Plus, Media Cybernetics Inc., USA).

2.5.3. Mechanical evaluation

Quasistatic tensile tests and dynamic loading cycles were carried out in a computer-controlled TA-TX Plus Texture Analyzer (Stable Micro Systems Ltd., Surrey, UK) equipped with a 5 kg load cell. For conventional quasistatic tensile tests, SDVG before and after functionalization were cut longitudinally, fixed between two grips with a gap of 10 mm, and subjected to uniaxial tensile stress at a rate of 0.1 mm/s. The tensile properties of each scaffold were tested, in triplicate, along both longitudinal and transversal axes. The tensile strength and the strain at break were calculated from the stress versus strain plots [7]. The Young's modulus was estimated from the initial slope of the engineering stress (force per area unit) versus the engineering strain (i.e., the strain minus the initial gap, referred to the initial gap).

Dynamic loading cycles were designed to mimic the internal pressure in a vascular graft and to evaluate the viscoelastic behavior under repeated pressures. The protocol was adapted from Stoiber et al. [41] with some modifications. The scaffold tubes were cut as rings of 3 mm height and loaded in circumferential direction in two U-like steel pins (1.5 mm diameter) that were respectively fixed to the up and down grips of the texturometer. Each sample was subjected to 20 cycles at a constant rate of 0.17 mm/s to a force of 0.080 N, and then to 20 cycles more to a force of 0.160 N. Other samples of each scaffold were subjected to 20 cycles to a force of 0.280 N at a rate of 0.33 mm/s. After the cycles all samples were subjected to uniaxial tensile stress at a rate of 0.17 mm/s until rupture. The forces of 0.080, 0.160, and 0.280 N were chosen to reproduce intraluminal pressures of 40, 80 and 140 mmHg according to Laplace's law

$$P = F / (2 \cdot r \cdot l)$$

where P is the luminal pressure, F is the applied force, r is the luminal radius of the scaffold, and l is the height (length) of the tubular piece [42]. All experiments were carried out at least in triplicate.

2.5.4. In vitro biological characterization

2.5.4.1. Cell culture and expansion

Human umbilical vein endothelial cells (HUVECs; ATCC® CRL-1730™) were cultured with F-12K Medium (Gibco) supplemented with 10% FBS (Corning), 0.1 mg/mL of heparin (Acros Organics) and 5 mL of endothelial cell growth supplement (ECGS; Sigma-Aldrich). Cells were cultured on tissue culture flaks at 37°C and 5% CO_2, changing the medium every day, and trypsinized with 0.25% (wt/v) Trypsin-EDTA solution when 80% confluent. All experiments were performed with passage 3.

2.5.4.2. Flow perfusion bioreactor set up and vascular graft preparation

A flow perfusion bioreactor was used for the culture of endothelial cells seeded vascular grafts to mimic physiological conditions. A WAVE rocking Bioreactor System (GE Healthcare Life Sciences GmbH, Spain) equipped with a Cellbag 2L, DOOPI VI, pHOPT and screwcap (GE Healthcare Life Sciences GmbH, Spain) was used as medium reservoir to monitor and control medium temperature, CO_2 percentage, O_2 percentage and pH during all the experiment. Complete endothelial cell culture media (2 L) was placed on the bag and warmed before starting the experiment.

Medium was pumped from the bag using a peristaltic pump and divided using adequate connectors to eight channels containing the grafts (four controls and four heparin-functionalized). The outlets were reconnected to a single tube and the medium was recirculated back into the bag. The perfusion achieved was 1.25 mL/min (0.11 cm/s) per line. This perfusion is comparable to the flow rates occurring in small diameter veins [43].

Control and functionalized vascular grafts were cut on 3 cm length sections and sterilized by 70% ethanol immersion for 30 min. Afterwards, grafts were assembled on the bioreactor system under sterile conditions leaving 1 cm length of the graft available for cell seeding. Grafts were then conditioned by the perfusion of 5 mL of complete endothelial cell culture medium to each of them and incubated at 37°C and 5% CO_2 for 12 h in static conditions.

2.5.4.3. SDVG seeding and culture

After graft conditioning, cell culture medium was removed, and each graft was seeded with 1 mL of endothelial cell suspension at 1 x 10^6 cells/mL in complete cell culture medium. Grafts were incubated in static conditions at 37°C and 5% CO_2 for 2 h, rotating them by 90° every 30 min. After this period, flow perfusion was started, and grafts were checked to remove bubbles and ensure stable flow. Finally, they were cultured under flow conditions for seven days checking them twice daily.

2.5.4.4. End point analysis

After one week of culture, grafts were collected and washed twice with 5 mL of DPBS (Gibco) without calcium and magnesium. Grafts were then cut into two pieces; 3 mm were fixed with 10% buffered formalin solution to assess cell morphology and attachment by confocal microscopy and the remaining 7 mm were immediately frozen at -80°C for gene expression analysis.

2.5.4.4.1. Cell morphology and attachment

The morphology and number of HUVECs attached on the surface of control and functionalized grafts were assessed by confocal microscopy. Cells were dyed with phalloidin-Alexa fluor 488 (Invitrogen) and DAPI (Invitrogen) using standard protocols and visualized using a confocal microscope (LEICA TCS-SP2). Confocal imaging using this approach (actin/nuclei staining) is commonly applied to evaluate endothelial cell adhesion and morphology onto several materials [44-48]. Cell surface area was obtained by image analysis of the maximum projections images by ImageJ (NIH).

2.5.4.4.2. Gene expression

The gene expression of endothelial cells grown on heparin functionalized SDVG and control SDVG was evaluated by Real-Time PCR Analysis. Total RNA was extracted from cells using an RNeasy Mini Kit (Quiagen) following the manufacturer's instructions. In brief, SDVGs were immersed in the supplied buffer and vortexed to lyse the cells. Then, SDVGs were removed, a QIAshredder spin column was used to homogenize the lysate, and ethanol was added before transfer to an RNeasy spin column. After three washes, total RNA was eluted adding 30 µL of RNAse-free water to the column membrane and spinning 2 min at 8000x g. RNA purity and concentration was measured in a Nanodrop 2000 (Thermo Fisher Scientific). RNA samples were reverse transcribed to cDNA according to the manufacturer's protocol (High Capacity cDNA Reverse Transcription Kit, Thermo Fisher Scientific). Thus, 10 µL of each purified total RNA was added to 10 µL of 2X reverse transcription master mix including 8 mM dNTP mix, RT Random primers, RNAse inhibitor and MultiScribeTM Reverse Transcriptase. Reverse transcription was performed in a thermo cycler using these conditions: 10 min at 25ºC, 120 min at 37ºC, and 5 min at 85ºC. Real-Time PCR was performed in a Quantstudio 12k Flex Applied Biosystems Cycler (Life Technologies) using the Fast SYBR Green Master Mix (Thermo Fisher Scientific). The genes of vascular endothelial growth factor receptor 2 (VEGFR2), Von Willebrand Factor (vWF) and Integrin α5 subunit were selected, and the human housekeeping gene RPL32 (Ribosomal Protein L32) was used as the reference transcript for all the PCR runs. In brief, to prepare the different Real-Time PCR reaction mixtures 1 µL of each cDNA templates and 5 µL of SYBR Green were employed, and final concentration of

forward/reverse primers was 0.5 μM. All conditions were tested in triplicate using these thermal cycling settings (fast mode): 2 min at 50ºC, 2 min at 95ºC, 40 cycles of 1 s at 95ºC, and 30 s at 60ºC. The Ct value for each sample was defined as the cycle number at which the fluorescence intensity reached a certain threshold. Relative gene expression level for each gene of interest was normalized by the Ct value of RPL32 using the 2ΔCt formula. Primers with the sequences depicted in Table 1 were purchased from Sigma-Aldrich at 0.25 μmol scale with desalt purification.

Table 1. Primer sequences used for Real-Time PCR analysis.

Primer	**Sequence**
VEGR2	F: GGAACCTCACTA[illegible]CCGCAGAGT
	R: CCAAGTTCGTCT[illegible]CCTGGGC
vWF	F: CCTTGAATCCC[illegible]GTGACCCTGA
	R: GGTTCCGAC[illegible]CTCCTCCACAT
Integrin-α5 subunit	F: GCCGATTC[illegible]CATCGCTCTCAAC
	R: GTCTTCTC[illegible]CAGTCCAGCAAG
RPL32	F: ACAAAG[illegible]CATGCTGCCCAGTG
	R: GCTCG[illegible]AGTACGACTACACTGAC

3. Results and Discussion

3.1. Surface modification of electrospun SDVG

In previous works we obtained tubular electrospun scaffolds with adequate degradation behavior and mechanical properties to be employed as SDVG [18,23,49,50]. Since antithrombogenic behavior as well as cell adhesion and proliferation ability are crucial for the success of these scaffolds, heparin grafting on flat surfaces has been explored applying different methodologies [35]. In the present work, bilayered SDVG were prepared with PLLA/PHD 50/50 wt/wt inner layer and PLLA/PHD 90/10 wt/wt external layer (0.24 mm total thickness). Synthesized PHD presented an intrinsic viscosity of 0.49 dL g^{-1}, and Mn and Mw values of 25.16 kg mol^{-1} and 58.47 kg mol^{-1} respectively, displaying a polydispersity index of 2.32. The inner surface of SDVG was modified with heparin through PHD urethane functional groups, which proved to be the most favorable route. As determined from toluidine blue colorimetric method, the density of immobilized heparin in the inner surface of SDVG was 9.1 ± 0.2 μg cm^{-2}. A neutral medium was employed for the determination because an acidic or alkaline medium would have led to PLLA hydrolysis, and thus to an overestimation of heparin functionalization values. This heparin density value was higher than others reported in literature for similar systems [30,31,40,51-53].

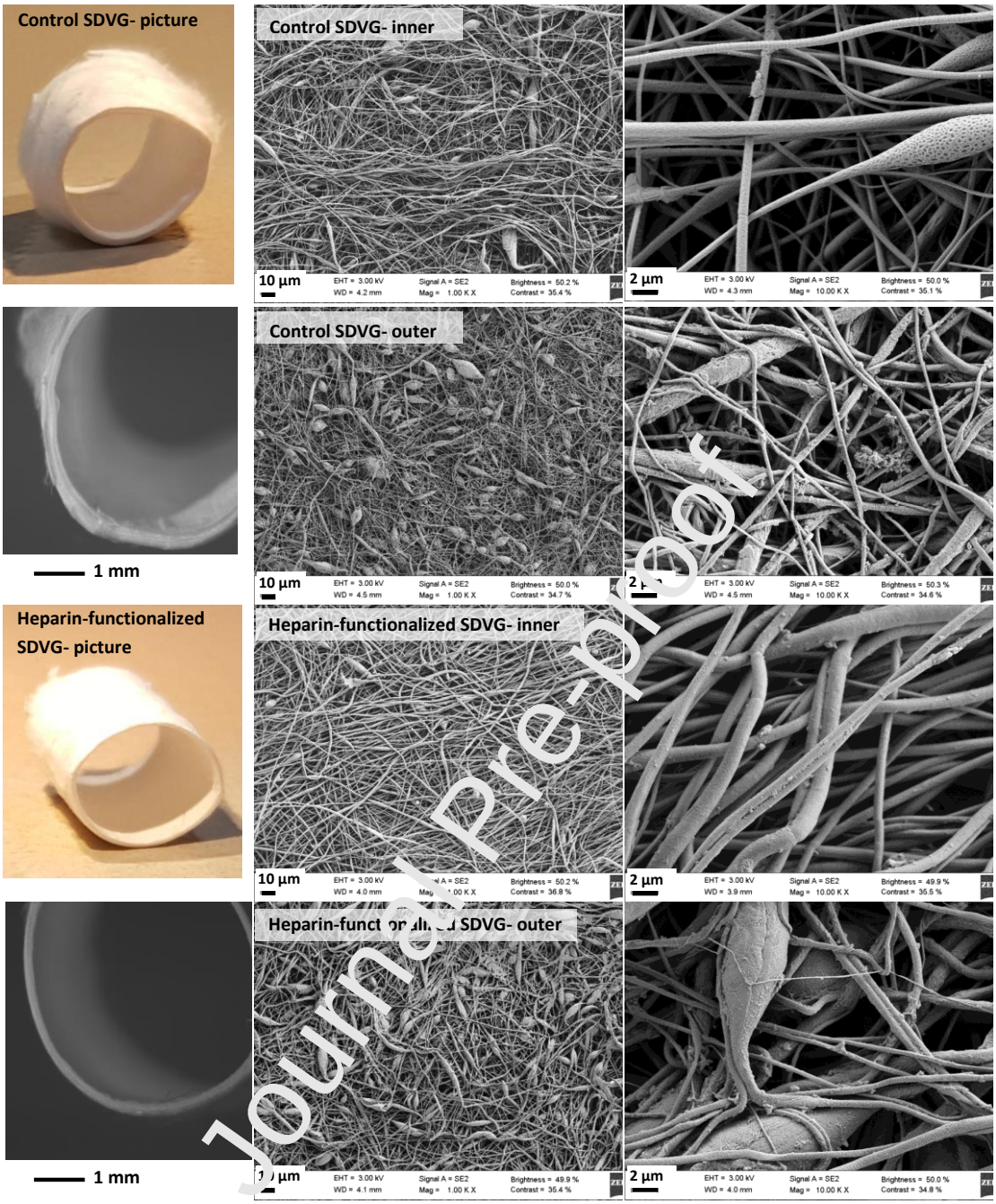

Figure 1. Optical images (first column) and SEM micrographs of control and heparin-immobilized SDVG. SEM micrographs of both inner and outer surfaces are shown at 1,000X (scale bar 10 µm) and 10,000X (scale bar 2 µm).

The microstructure of the SDVG before (control) and after heparin immobilization (functionalized) is shown in Figure 1. The mean fiber diameters for the inner and outer layers were 511 ± 306 nm and 734 ± 374 nm, respectively. After heparin modification, the obtained values were 638 ± 310 nm and 591 ± 302 nm, respectively. Thus, no significant differences in fiber diameter due to the modification procedure could be appreciated. The inner surface was

formed by quite uniform nanofibers, while the outer layer consisted in more beaded fibers and with wider diameter size dispersion. This finding is in good agreement with previous reports showing that PHD requires quite high concentration to produce bead-free fibers [18].

3.2. Mechanical behavior

Quasistatic tensile tests revealed that control SDVG present anisotropic tensile behavior. The electrospun scaffolds were longitudinally cut and the tensile properties recorded along longitudinal and transversal axes (Figure 2; Table 2). Along the longitudinal axis control SDVG had higher tensile strength (2.60 MPa, s.d. <10%) and Young's modulus (20.5 MPa; s.d. 1.1) than along the transversal axis (2.27 MPa, s.d. <10%; and 7.8 MPa, s.d. 0.1). Once the maximum tensile strength was reached, the control SDVG frayed progressively instead of tearing, which explains the slow decay of the tensile strength. This behavior may be related to the fact that SDVG are formed by two different layers which exhibit different mechanical properties; PLLA/PHD 90/10 wt/wt external layer having higher modulus [50]. Interestingly, after immobilization of heparin the functionalized SDVG showed enhanced tensile strength along the transversal axis (3.65 MPa, s.d. <10%) compared to the longitudinal axis (2.83 MPa, s.d. <10%) and, thus, the Young's modulus in both longitudinal (21.3 MPa, s.d. 2.3) and transversal (24.0 MPa, s.d. 1.6) axes became more similar. The functionalization may have introduced additional links between the two layers, preventing SDVG from disassemble under strong stress. The tensile strength of functionalized SDVG was higher than that reported for protein-based scaffolds [7], PLLA electrospun grafts [50] and PLLA / poly(L-lactide-co-ε-caprolactone) (PLCL) porous grafts obtained by thermally induced phase separation (TIPS) [54], and compared quite well with that of human saphenous vein (the most commonly used autograft vessel) in both directions [55] and with electrospun grafts made of poly(ε-caprolactone) [9].

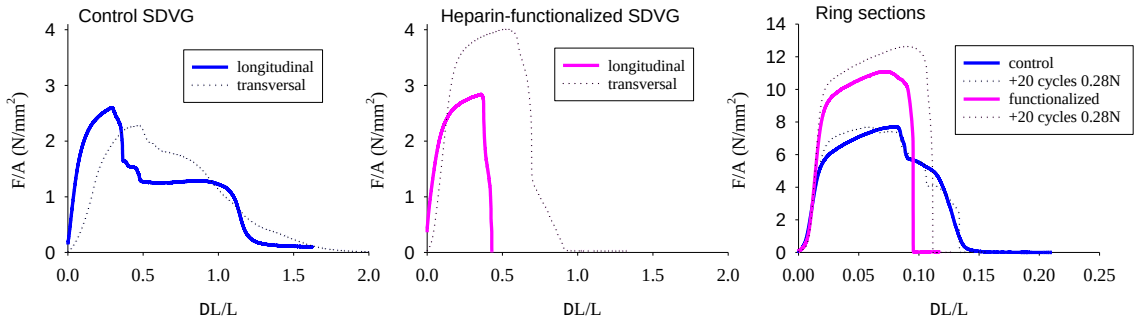

Figure 2. Engineering stress versus engineering strain plots recorded along longitudinal and transversal axes for control and heparin-functionalized SDVG, and recorded for ring sections of control and heparin-functionalized SDVG before and after 20 cycles of dynamic loading at 0.280 N.

Since vascular grafts should perform as viscoelastic materials able to withstand physiological pressures, mechanical behavior under dynamic loading cycles at forces of 0.08, 0.16 and 0.28 N that resemble pressures of 40, 80 and 140 mmHg was investigated [41,42]. As depicted in Figure 3, the ring sections of the scaffolds showed a nearly perfect elastic performance, with symmetric peaks and reproducible areas from the second to the last peak in each cycle. The first peak data started to be recorded at 0.01 N, which was set as the activation force.

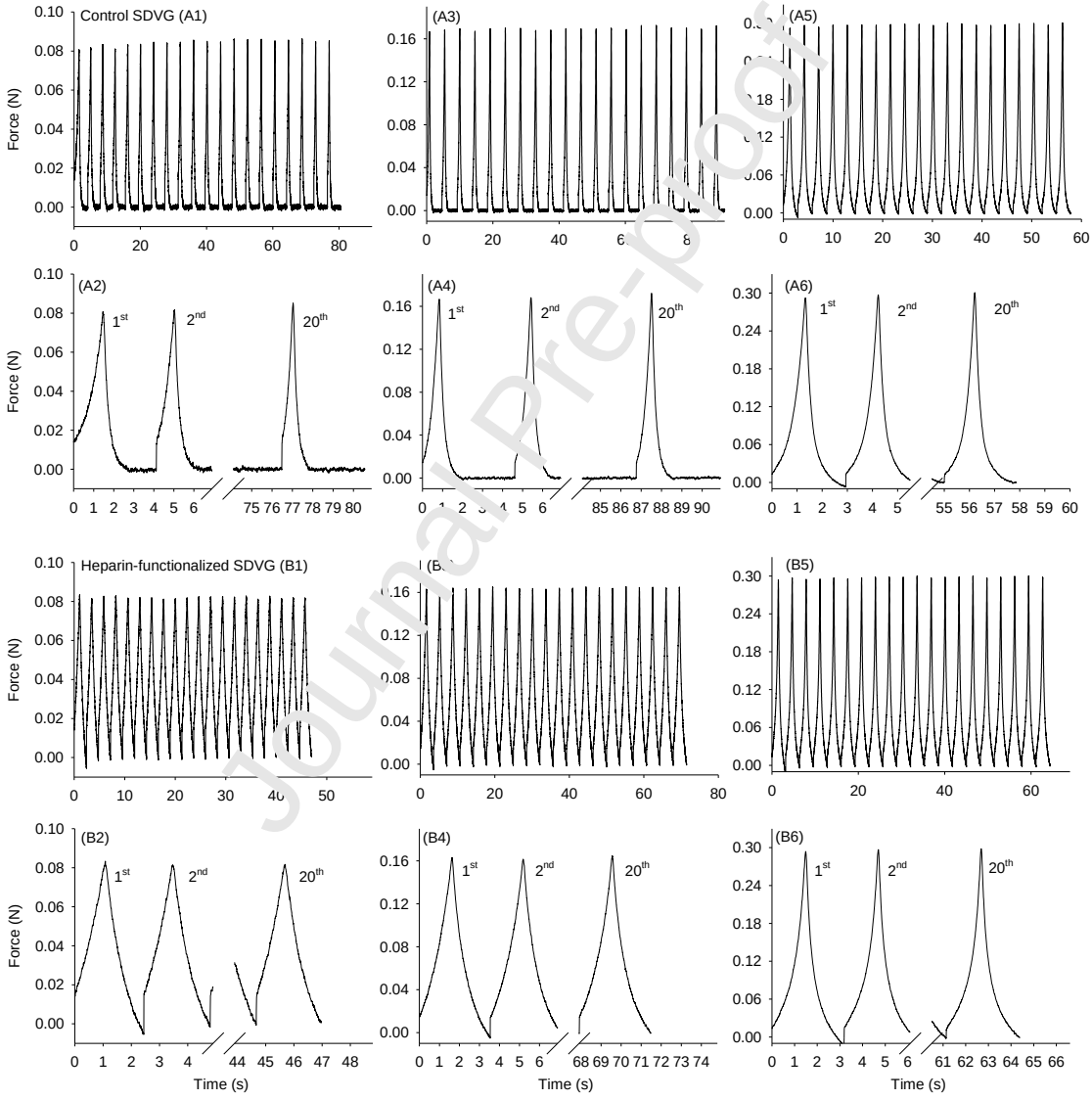

Figure 3. Stress-strain behavior of control SDVG and heparin-functionalized SDVG recorded under dynamic loading cycles at forces of 0.080 N (A1, A2, B1, B2), 0.160 N (A3, A4, B3, B4) or 0.280 N (A5, A6, B5, B6). Peaks corresponding to the 1st, 2nd, and 20th cycle are shown in detail in even plots.

In the dynamic loading, control SDVG rings showed minor changes in peak areas along the cycles, as depicted in Table 2. The decrease in area suggested material compaction as cycles proceeded, and the energy involved in the cycle decreased. Differently, heparin-functionalized SDVG rings did not show any change along the 20 cycles, even when subjected to the highest force and a faster stress (0.33 mm/s instead of 0.17 mm/s). Also in good agreement with the quasistatic tensile tests, heparin-functionalized SDVG rings tested until rupture (Figure 2) showed higher tensile stress and sharp break, while control SDVG rings frayed progressively, starting from the inner layer. The tests of the scaffold samples as rings placed in the U-supports revealed elongations at break of 13-15% for control SDVG and 9.5-11% for the functionalized SDVG, which are close to those recorded for human saphenous vein (11-17%) [55]. Relevantly, the slopes in the initial region of the stress-strain plots (Figure 2) were similar for freshly prepared rings and for rings that had already underwent the 20-cycle processing even at the higher loading stress. This suggests that no relevant changes in the Young's moduli occurred after dynamic loading test mimicking physiological conditions.

Table 2. Stress-strain areas recorded for control and functionalized SDVG scaffolds under dynamic loading cycles, and differences in areas recorded between the 2nd and the 20th peaks. Rings (3 mm height) were loaded at a constant rate of 0.17 mm/s to forces of 0.080 and 0.016 N, and at a constant rate of 0.33 mm/s to a force of 0.028 N. Mean values and, in parenthesis, standard deviation (n=3 for three independent measurements).

Scaffold	Force (N)	$Area_{Peak2}$ (N·mm)	$Area_{Peak20}$ (N·mm)	ΔArea (%)
Control	0.080	0.010 (0.001)	0.008 (0.001)	14.9 (14.1)
	0.016	0.020 (0.004)	0.019 (0.004)	5.0 (3.3)
	0.028	0.064 (0.004)	0.059 (0.004)	7.5 (0.1)
Functionalized	0.080	0.019 (0.004)	0.019 (0.004)	0.1 (1.0)
	0.016	0.043 (0.006)	0.042 (0.005)	1.4 (1.2)
	0.028	0.077 (0.020)	0.076 (0.020)	1.0 (0.8)

3.3. Cell morphology and attachment

To gain further insight into the performance of the heparin-immobilized scaffolds for replacement of small-diameter blood vessels, HUVECs culture, adhesion and proliferation were studied. Figure 4 shows the morphology of HUVECs grown on both functionalized and control SDVG. The incorporation of heparin to the grafts surface increased not only the total number of attached cells but also their spreading on the surface. In agreement with this, the cumulative surface area of the grafts covered by cells after seven days of culture was clearly higher on the

constructs functionalized with heparin as shown in Figure 5. The common use of heparin as anticoagulant relies on its binding to antithrombin via a specific pentasaccharide sequence [56]. Heparin solely has been barely investigated to functionalize vascular grafts to promote cell attachment, although it may serve as linker to incorporate several growth factors as vascular endothelial growth factor (VEGF) or basic fibroblast growth factor (bFGF) crucial in angiogenesis [57,58]. This use of heparin is based on its affinity to bind different proteins through its sulfate motifs that function as molecular recognition elements for growth factors [59]. Consequently, the presence of heparin on the SDVG surface could lead to the attachment of several growth factors of those included on the cell culture medium used for the experiment. The incorporation of growth factors together with the presence of heparin would then promote cell attachment and proliferation while ensuring excellent hemocompatibility [35]. In this regard, the incorporation of heparin to our vascular grafts increased six-fold the surface area colonized by cells after seven days of culture under flow conditions when compared to control SDVG (Figure 5). Similarly, Shi and coworkers reported a significant increase in graft endothelialization *in vivo* in a rat model for electrospun PCL/gelatin loaded with heparin compared to non-loaded ones [60]. Moreover, the heparin surface modification of silk fibroin / PLLA and PLGA / PLLA / PLCL grafts led to an increase in HUVECs attachment, proliferation and migration [61,62]. Also in good agreement, the addition of heparin to modified PTFE grafts was shown to increase HUVECs proliferation compared to grafts without heparin [63].

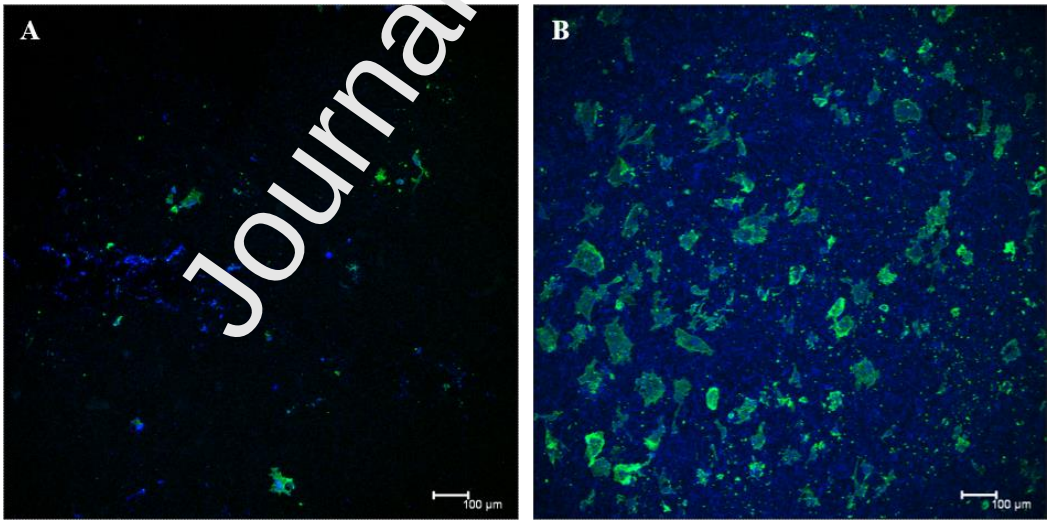

Figure 4. Confocal micrographs of representative fields of A) pristine SDVG and B) heparin-functionalized SDVG at 10X magnification. Adhered HUVECs were stained with phalloidin-Alexa fluor 488 (green; cytoplasm) and DAPI (blue; nucleus). Scale bars: 100 µm.

Journal Pre-proof

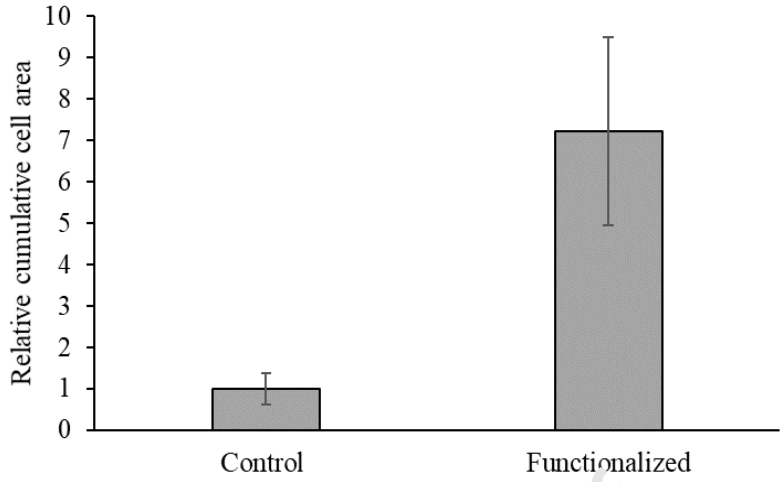

Figure 5. Relative surface area occupied by HUVECs grown on heparin-functionalized SDVG with respect to pristine SDVG (control).

3.4. HUVECs gene expression analysis

The response of endothelial cells subjected to shear stress by laminar flow during seven days on the developed biomaterials was assessed by quantitative Real-Time PCR (Figure 6). Two genes associated with endothelium functionality, namely hemostasis (vWF) and angiogenesis (VEGFR2), were selected to evaluate cell performance [64,65]. Moreover, the gene expression of a protein associated with cell migration under shear stress, integrin α5 subunit, was also analyzed [66].

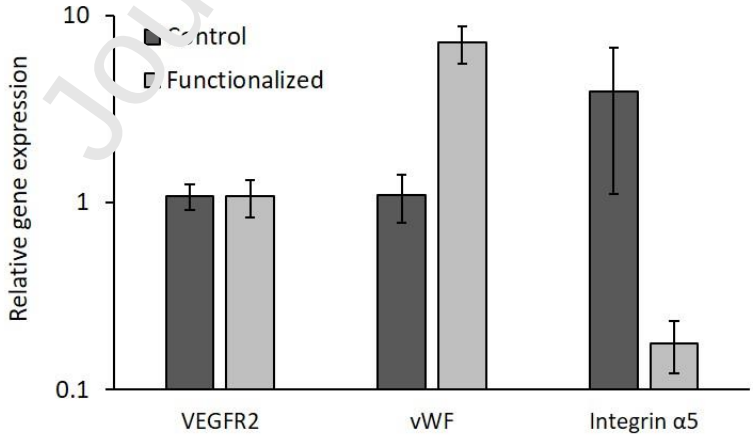

Figure 6. Relative gene expression of HUVECs cultured on the surface of control and heparin-functionalized SDVG after seven days in culture under laminar flow.

Journal Pre-proof

Endothelial cells gene expression normalized by the housekeeping gene RPL32 is shown in Figure 6. Despite the differences displayed in cell spreading and morphology, no differences on VEGFR2 gene expression were observed. However, the expression of vWF was clearly upregulated for cells cultured on heparin-functionalized SDVG when compared to control grafts. Similarly to our findings, Lekesiz et al. [67] have pointed out the ability of heparin to induce vWF secretion by HUVECs in a dose dependent manner when added in solution to the cell culture media. Moreover, HUVECs cultured on heparin-modified ePTFE vascular grafts expressed the endothelial cell-specific marker vWF [68] and *in vivo* assessments have described the capacity of a heparinized stent to increase vWF gene expression on the myocardial tissue around the stent when compared to the bare stent [69]. Functional endothelial cells secrete vWF controlling the hemostatic process by its mediation in platelet adhesion and aggregation and carrying coagulation factor VIII in the circulation [70]. The use of heparin-functionalized SDVG could avoid the intrinsic thrombogenicity of vascular prostheses as we previously reported [35] and encourage the recovery of the endothelium homeostasis by promoting vWF expression.

On the other hand, the expression of integrin α5 subunit was decreased on endothelial cells grown on heparin-functionalized SDVG after 7 days of culture. Integrin α5 subunit has been reported to be crucial in endothelial cell migration when subjected to shear stress and therefore, its expression is directly correlated to cell migration under these conditions [71]. Interestingly, our findings indicate a reduction in the gene expression of this protein on functionalized grafts. The increased cell spreading on these grafts would provide enhanced cell attachment promoting biomaterial engraftment and leading to a decrease in migration [46].

4. Conclusions

In this work, the inner surface of PLLA/PHD electrospun tubular scaffolds was successfully modified with heparin through PHD urethane functionalization. Interestingly, functionalization of SDVG with heparin improved the tensile properties and promoted stable and functional endothelial cell attachment. This newly designed biodegradable SDVG avoids the need of further addition of growth factors during the scaffold preparation, leading to more cost-effective and stable vascular grafts with excellent biological performance.

Acknowledgements

This work was supported by CONICET [PIP 153/2017], UNMdP 15/G479 (Argentina), Interreg V-A POCTEP Program [0245_IBEROS_1_E], MINECO [SAF2017-83118-R, and Innopharma Project], Agencia Estatal de Investigación (AEI) Spain, Xunta de Galicia [ED431C 2018/21, ED431C 2020/17] and European Regional Development Fund (FEDER).

5. References

[1] E.J. Benjamin, M.J. Blaha, S.E. Chiuve, M. Cushman, S.R. Das, R. Deo, S.D. de Ferranti, J. Floyd, M. Fornage, C. Gillespie, C.R. Isasi, M.C. Jiménez, L.C. Jordan, S.E. Judd, D. Lackland, J.H. Lichtman, L. Lisabeth, S. Liu, C.T. Longenecker, R.H. Mackey, K. Matsushita, D. Mozaffarian, M.E. Mussolino, K. Nasir, R.W. Neumar, I. Palaniappan, D.K. Pandey, R.R. Thiagarajan, M.J. Reeves, M. Ritchey, C.J. Rodriguez, G.A. Roth, W.D. Rosamond, C. Sasson, A. Towfighi, C.W. Tsao, M.B. Turner, S.S. Virani, J.H. Voeks, J.Z. Willey, J.T. Wilkins, J.H.Y. Wu, H.M. Alger, S.S. Wong, P. Muntner, Heart disease and stroke statistics-2017 update: A report from the American Heart Association, Circulation 135 (2017) e146–e603. https://doi.org/10.1161/CIR.0000000000000485.

[2] D.G. Seifu, A. Purnama, K. Mequanint, D. Mantovani, Small-diameter vascular tissue engineering, Nat. Rev. Cardiol. 10 (2013) 410–421. https://doi.org/10.1038/nrcardio.2013.77.

[3] N. L'Heureux, N. Dusserre, G. Konig, B. Victor, P. Keire, T.N. Wight, N.A.F. Chronos, A.E. Kyles, C.R. Gregory, G. Hoyt, R.C. Robbins, T.N. McAllister, Human tissue-engineered blood vessels for adult arterial revascularization, Nat. Med. 12 (2006) 361–365. https://doi.org/10.1038/nm1364.

[4] H.J. Salacinski, S. Goldner, A. Giudiceandrea, G. Hamilton, A.M. Seifalian, A. Edwards, R.J. Carson, The mechanical behavior of vascular grafts: a review, J. Biomater. Appl. 15 (2001) 241–278. https://doi.org/10.1106/NA5T-J57A-JTDD-FD04.

[5] S.S. Gisbertz, R.P. Tutein Nolthenius, G.J. de Borst, L. van der Laan, T.T. Overtoom, F.L. Moll, J.P.P.M. de Vries, Remote endarterectomy versus supragenicular bypass surgery for long occlusions of the superficial femoral artery: medium-term results of a randomized controlled

trial (the REVAS trial), Ann. Vasc. Surg. 24 (2010) 1015–1023. https://doi.org/10.1016/j.avsg.2010.03.022.

[6] J. Chlupác, E. Filová, L. Bacáková, Blood vessel replacement: 50 years of development and tissue engineering paradigms in vascular surgery, Physiol. Res. 58 (2009) Suppl 2 S119–139.

[7] V. Catto, S. Fare, I. Cattaneo, M. Figliuzzi, A. Alessandrino, G. Freddi, A. Remuzzi, M.C. Tanzi, Small diameter electrospun silk fibroin vascular grafts: Mechanical properties, in vitro biodegradability, and in vivo biocompatibility, Mater. Sci. Eng. C Mater. Biol. Appl. 54 (2015) 101–111. https://doi.org/10.1016/j.msec.2015.05.003.

[8] I. Sipahi, M.H. Akay, S. Dagdelen, A. Blitz, C. Alhan, Coronary artery bypass grafting vs percutaneous coronary intervention and long-term mortality and morbidity in multivessel disease: meta-analysis of randomized clinical trials of the arterial grafting and stenting era, JAMA Intern. Med. 174 (2014) 223–230. https://doi.org/10.1001/jamainternmed.2013.12844.

[9] S. de Valence, J.C. Tille, D. Mugnai, W. Mrowczynski, R. Gurny, M. Moller, B.H. Walpoth, Long term performance of polycaprolactone vascular grafts in a rat abdominal aorta replacement model, Biomaterials 33 (2012) 38–47. https://doi.org/10.1016/j.biomaterials.2011.09.024.

[10] Y. Hong, S.H. Ye, A. Nieponice, L. Soletti, D.A. Vorp, W.R. Wagner, A small diameter, fibrous vascular conduit generated from a poly(ester urethane)urea and phospholipid polymer blend, Biomaterials 30 (2009) 2457–2467. https://doi.org/10.1016/j.biomaterials.2009.01.013.

[11] W. Zheng, Z. Wang, L. Song, Q. Zhao, J. Zhang, D. Li, S. Wang, J. Han, X.L. Zheng, Z. Yang, D. Kong, Endothelialization and patency of RGD-functionalized vascular grafts in a rabbit carotid artery model, Biomaterials 33 (2012) 2880–2891. https://doi.org/10.1016/j.biomaterials.2011.12.047.

[12] D.E. Muylaert, J.O. Fledderus, C.V. Bouten, P.Y. Dankers, M.C. Verhaar, Combining tissue repair and tissue engineering; bioactivating implantable cell-free vascular scaffolds, Heart (British Cardiac Society) 100 (2014) 1825–1830. https://doi.org/10.1136/heartjnl-2014-306092.

[13] A. Post, P. Diaz-Rodriguez, B. Balouch, S. Paulsen, S. Wu, J. Miller, M. Hahn, E. Cosgriff-Hernandez, Elucidating the role of graft compliance mismatch on intimal hyperplasia using an ex vivo organ culture model, Acta Biomater. 89 (2019) 84–94. https://doi.org/10.1016/j.actbio.2019.03.025.

[14] F. Chen, X. Li, X. Mo, C. He, H. Wang, Y. Ikada, Electrospun chitosan-P(LLA-CL) nanofibers for biomimetic extracellular matrix, J. Biomater. Sci. Polym. Ed. 19 (2008) 677–691. https://doi.org/10.1163/156856208784089661,

[15] T.J. Sill, H.A. von Recum, Electrospinning: applications in drug delivery and tissue engineering, Biomaterials 29 (2008) 1989–2006. https://doi.org/10.1016/j.biomaterials.2008.01.011.

[16] Y.M. Ju, J.S. Choi, A. Atala, J.J. Yoo, S.J. Lee, Bilayered scaffold for engineering cellularized blood vessels, Biomaterials 31 (2010) 4313–4321. https://doi.org/10.1016/j.biomaterials.2010.02.002.

[17] D.K. Patel, K.T. Lim, 2019. Biomimetic polymer-based engineered scaffolds for improved stem cell function. Materials (Basel) 12, 2950. https://doi.org/10.3390/ma12182950.

[18] F. Montini Ballarin, P.C. Caracciolo, E. Blotta, V.L. Ballarin, G.A. Abraham, Optimization of poly(L-lactic acid)/segmented polyurethane electrospinning process for the production of bilayered small-diameter nanofibrous tubular structures, Mater. Sci. Eng. C Mater. Biol. Appl. 42 (2014) 489–499. https://doi.org/10.1016/j.msec.2014.05.074.

[19] M.A. Lillie, T.E. Armstrong, S.G. Gerard, R.E. Shadwick, J.M. Gosline, Contribution of elastin and collagen to the inflation response of the pig thoracic aorta: assessing elastin's role in mechanical homeostasis, J. Biomech. 45 (2012) 2133–2141. https://doi.org/10.1016/j.jbiomech.2012.05.034.

[20] M.R. Roach, A.C. Burton, The reason for the shape of the distensibility curves of arteries, Can. J. Biochem. Physiol. 35 (1957) 681–690.

[21] P.C. Caracciolo, F. Buffa, G.A. Abraham, Effect of the hard segment chemistry and structure on the thermal and mechanical properties of novel biomedical segmented poly(esterurethanes), J. Mater. Sci. Mater. Med. 20 (2009) 145–155. https://doi.org/10.1007/s10856-008-3561-8.

[22] P.C. Caracciolo, V. Thomas, Y.K. Vohra, F. Buffa, G.A. Abraham, Electrospinning of novel biodegradable poly(ester urethane)s and poly(ester urethane urea)s for soft tissue-engineering applications, J. Mater. Sci. Mater. Med. 20 (2009) 2129–2137. https://doi.org/10.1007/s10856-009-3768-3.

[23] F. Montini-Ballarin, D. Suárez-Bagnasco, L.J. Cymberknop, C. Balay, P.C. Caracciolo, C. Negreira, R.L. Armentano, G.A. Abraham, Elasticity response of electrospun bioresorbable small-diameter vascular grafts: Towards a biomimetic mechanical response, Mater. Lett. 209 (2017) 175–177. https://doi.org/10.1016/j.matlet.2017.07.110.

[24] G.M. Fischer, J.G. Llaurado, Collagen and elastin content in canine arteries selected from functionally different vascular beds, Circ. Res. 19 (1966) 394–399. https://doi.org/10.1161/01.res.19.2.394.

[25] J.A.G. Rhodin, Architecture of the vessel wall, in: American Physiological Society (Ed.), Comprehensive Physiology, John Wiley & Sons Inc., New York, 2011, pp. 1–31. https://doi.org/10.1002/cphy.cp020201.

[26] H. Sonoda, K. Takamizawa, Y. Nakayama, H. Yasui, T. Matsuda, Small-diameter compliant arterial graft prosthesis: Design concept of coaxial double tubular graft and its fabrication, J. Biomed. Mater. Res. 55 (2001) 266–276. https://doi.org/10.1002/1097-4636(20010605)55:3<266::aid-jbm1014>3.0.co;2-c.

[27] E.M. Srokowski, P.H. Blit, W.G. McClung, J.L. Brash, J.P. Santerre, K.A. Woodhouse, Platelet adhesion and fibrinogen accretion on a family of elastin-like polypeptides, J. Biomater. Sci. Polym. Ed. 22 (2011) 41–57. https://doi.org/10.1163/092050609X12578498935594.

Journal Pre-proof

[28] X. Ren, Y. Feng, J. Guo, H. Wang, Q. Li, J. Yang, X. Hao, J. Lv, N. Ma, W. Li, Surface modification and endothelialization of biomaterials as potential scaffolds for vascular tissue engineering applications, Chem. Soc. Rev. 44 (2015) 5680–5742. https://doi.org/10.1039/c4cs00483c.

[29] G. Altankov, V. Thom, T. Groth, K. Jankova, G. Jonsson, M. Ulbricht, Modulating the biocompatibility of polymer surfaces with poly(ethylene glycol): effect of fibronectin, J. Biomed. Mater. Res. 52 (2000) 219–230. https://doi.org/10.1002/1097-4636(200010)52:1<219::aid-jbm28>3.0.co;2-f.

[30] Y.K. Joung, I.K. Hwang, K.D. Park, C.W. Lee, CD34 monoclonal antibody-immobilized electrospun polyurethane for the endothelialization of vascular grafts, Macromol. Res. 18 (2010) 904–912. https://doi.org/10.1007/s13233-010-0908-z.

[31] Y. Feng, H. Tian, M. Tan, P. Zhang, Q. Chen, J. Liu, Surface modification of polycarbonate urethane by covalent linkage of heparin with a PEG spacer, Trans. Tianjin Univ. 19 (2013) 58–65. https://doi.org/10.1007/s12209-013-1894-y.

[32] J. Zhang, J. Wang, Y. Wei, C. Gao, X. Chen, W. Kong, D. Kong, Q. Zhao, ECM-mimetic heparin glycosamioglycan-functionalized surface favors constructing functional vascular smooth muscle tissue in vitro, Colloids Surf. B Biointerfaces 146 (2016) 280–288. https://doi.org/10.1016/j.colsurfb.2016.06.023.

[33] I.S. Robu, H.L. Walters 3rd, H.W.T. Matthew, Morphological and growth responses of vascular smooth muscle and endothelial cells cultured on immobilized heparin and dextran sulfate surfaces, J. Biomed. Mater. Res. Part A 105 (2017) 1725–1735. https://doi.org/10.1002/jbm.a.36037.

[34] K. Gasowska, B. Naumnik, K. Klejna, M. Mysliwiec, The influence of unfractionated and low-molecular weight heparins on the properties of human umbilical vein endothelial cells (HUVEC), Folia Histochem. Cytobiol. 47 (2009) 17–23. https://doi.org/10.2478/v10042-009-0008-0.

Journal Pre-proof

[35] P.C. Caracciolo, M.I. Rial-Hermida, F. Montini-Ballarin, G.A. Abraham, A. Concheiro, C. Alvarez-Lorenzo, Surface-modified bioresorbable electrospun scaffolds for improving hemocompatibility of vascular grafts, Mater. Sci. Eng. C Mater. Biol. Appl. 75 (2017) 1115–1127. https://doi.org/10.1016/j.msec.2017.02.151.

[36] Q. Lu, S. Zhang, K. Hu, Q. Feng, C. Cao, F. Cui, Cytocompatibility and blood compatibility of multifunctional fibroin/collagen/heparin scaffolds, Biomaterials 28 (2007) 2306–2313. https://doi.org/10.1016/j.biomaterials.2007.01.031.

[37] P. Klement, Y.J. Du, L. Berry, M. Andrew, A.K. Chan, Blood compatible biomaterials by surface coating with a novel antithrombin-heparin covalent complex, Biomaterials 23 (2002) 527–535. https://doi.org/10.1016/s0142-9612(01)00135-1.

[38] G. Pitarresi, C. Fiorica, F.S. Palumbo, S. Rigogliuso, G. Ghersi, G. Giammona, Heparin functionalized polyaspartamide/polyester scaffold for potential blood vessel regeneration, J. Biomed. Mater. Res. Part A 102 (2014) 1334–1341. https://doi.org/10.1002/jbm.a.34818.

[39] S. Liu, C. Dong, G. Lu, Q. Lu, Z. Li, D.L. Kaplan, H. Zhu, Bilayered vascular grafts based on silk proteins, Acta Biomater. 9 (2013) 8991–9003. https://doi.org/10.1016/j.actbio.2013.06.045.

[40] Q. Cheng, K. Komvopoulos, S. Li, Plasma-assisted heparin conjugation on electrospun poly(L-lactide) fibrous scaffolds, J. Biomed. Mater. Res. Part A 102 (2014) 1408–1414. https://doi.org/10.1002/jbm.a.34802.

[41] M. Stoiber, C. Grasl, K. Frieberger, F. Moscato, H. Bergmeister, H. Schima, Impact of the testing protocol on the mechanical characterization of small diameter electrospun vascular grafts, J. Mech. Behav. Biomed. Mater. 104 (2020) 103652. https://doi.org/10.1016/j.jmbbm.2020.103652.

[42] H. Bergmeister, C. Schreiber, C. Grasl, I. Walter, R. Plasenzotti, M. Stoiber, D. Bernhard, H. Schim, Healing characteristics of electrospun polyurethane grafts with various porosities, Acta Biomater. 9 (2013) 6032–6040. https://doi.org/10.1016/j.actbio.2012.12.009.

[43] M. Klarhöfer, B. Csapo, C. Balassy, J.C. Szeles, E. Moser, High-resolution blood flow velocity measurements in the human finger, Magn. Reson. Med. 45 (2001) 716–719. https://doi.org/10.1002/mrm.1096.

[44] L.A. Dudash, F. Kligman, S.M. Sarett, K. Kottke-Marchant, R.E. Marchant, Endothelial cell attachment and shear response on biomimetic polymer-coated vascular grafts, J. Biomed. Mater. Res. Part A 100 (2012) 2204–2210. https://doi.org/10.1002/jbm.a.34119.

[45] N.F. Huang, J. Okogbaa, J.C. Lee, A. Jha, T.S. Zaitseva, M.V. Paukshto, J.S. Sun, N. Punjya, G.G. Fuller, J.P. Cooke, The modulation of endothelial cell morphology, function, and survival using anisotropic nanofibrillar collagen scaffolds, Biomaterials 34 (2013) 4038–4047. https://doi.org/10.1016/j.biomaterials.2013.02.036.

[46] J.F. Diaz Quiroz, P. Diaz Rodriguez, J.D. Erndt-Marino, V. Guiza, B. Balouch, T. Graf, W.M. Reichert, B. Russell, M. Höök, M.S. Hahn, Collagen-mimetic proteins with tunable integrin binding sites for vascular graft coatings, ACS Biomater. Sci. Eng. 4 (2018) 2934–2942. https://doi.org/10.1021/acsbiomaterials.8b00070.

[47] J.-L. Wang, K.-F. Ren, H. Chang, F. Jia, B.-C. Li, Y. Ji, J. Ji, Direct Adhesion of Endothelial Cells to Bioinspired Poly(dopamine) Coating Through Endogenous Fibronectin and Integrin α5β1, Macromol. Biosci. 13 (2013) 483–493. https://doi.org/10.1002/mabi.201200390.

[48] W. Jiang, C. Zhang, L. Tran, S.G. Wang, A.D. Hakim, H. Liu, Engineering Nano-to-Micron-Patterned Polymer Coatings on Bioresorbable Magnesium for Controlling Human Endothelial Cell Adhesion and Morphology, ACS Biomater. Sci. Eng. 6 (2020) 3878–3898. https://doi.org/10.1021/acsbiomaterials.0c00642.

[49] F. Montini-Ballarin, P.C. Caracciolo, G. Rivero, G.A. Abraham, In vitro degradation of electrospun poly(L-lactic acid)/segmented poly(ester urethane) blends, Polym. Degrad. Stabil. 126 (2016) 159–169. https://doi.org/10.1016/j.polymdegradstab.2016.02.007.

[50] F. Montini-Ballarin, D. Calvo, P.C. Caracciolo, F. Rojo, P.M. Frontini, G.A. Abraham, G.V. Guinea, Mechanical behavior of bilayered small-diameter nanofibrous structures as

biomimetic vascular grafts, J. Mech. Behav. Biomed. Mater. 60 (2016) 220–233. https://doi.org/10.1016/j.jmbbm.2016.01.025.

[51] R.R.R. Janairo, J.J.D. Henry, B.L.P. Lee, C.K. Hashi, N. Derugin, R. Lee, S. Li, Heparin-modified small-diameter nanofibrous vascular grafts, IEEE Trans. Nanobiosci. 11 (2012) 22–27. https://doi.org/10.1109/TNB.2012.2188926.

[52] I.S. Alferiev, J.M. Connolly, S.J. Stachelek, A. Ottey, L. Rauova, R.J. Levy, Surface heparinization of polyurethane via bromoalkylation of hard segment nitrogens, Biomacromolecules 7 (2006) 317–322. https://doi.org/10.1021/bm050696694.

[53] T.W. Chuang, K.S. Masters, Regulation of polyurethane hemocompatibility and endothelialization by tethered hyaluronic acid oligosaccharides, Biomaterials 30 (2009) 5341–5351. https://doi.org/10.1016/j.biomaterials.2009.06.029.

[54] W. Wang, J. Hu, C. He, W. Nie, W. Feng, K. Qin, X. Zhou, Y. Gao, G. Wang, Heparinized PLLA/PLCL nanofibrous scaffold for potential engineering of small-diameter blood vessel: Tunable elasticity and anticoagulation property, J. Biomed. Mater. Res. Part A 103 (2015) 1784–1797. https://doi.org/10.1002/jbm.a.35315.

[55] D.L. Donovan, S.P. Schmidt, S.P. Townshend, G.O. Njus, W.V. Sharp, Material and structural characterization of human saphenous vein, J. Vasc. Surg. 12 (1990) 531–537.

[56] M. Kolar, M. Mozetič, K. Stana-Kleinschek, M. Fröhlich, B. Turk, A. Vesel, Covalent binding of heparin to functionalized PET materials for improved haemocompatibility, Materials (Basel) 8 (2015) 1526–1544. https://doi.org/10.3390/ma8041526.

[57] J.C. Wu, H.C. Yan, W.T. Chen, W.H. Chen, C.J. Wang, Y.C. Chi, W.Y. Kao, JNK signaling pathway is required for bFGF-mediated surface cadherin downregulation on HUVEC, Exp. Cell Res. 314 (2008) 421–429. https://doi.org/10.1016/j.yexcr.2007.10.002.

[58] C. Liu, Y. Liu, J. He, R. Mu, Y. Di, N. Shen, X. Liu, X. Gao, J. Wang, T. Chen, T. Fang, H. Li, F. Tian, 2019. Liraglutide increases VEGF expression via CNPY2-PERK pathway

induced by hypoxia/reoxygenation injury. Front. Pharmacol. 10, 789. https://doi.org/10.3389/fphar.2019.00789.

[59] M. Tallawi, E. Rosellini, N. Barbani, M.G. Cascone, R. Rai, G. Saint-Pierre, A.R. Boccaccini, 2015. Strategies for the chemical and biological functionalization of scaffolds for cardiac tissue engineering: a review. J. R. Soc. Interface. 12, 20150254. https://doi.org/10.1098/rsif.2015.0254.

[60] J. Shi, S. Chen, L. Wang, X. Zhang, J. Gao, L. Jiang, D. Tang, L. Zhang, A. Midgley, D. Kong, S. Wang, Rapid endothelialization and controlled smooth muscle regeneration by electrospun heparin-loaded polycaprolactone/gelatin hybrid vascular grafts, J. Biomed. Mater. Res. Part B 107 (2019) 2040–2049. https://doi.org/10.1002/jbm.b.34295.

[61] H.-Y. Mi, X. Jing, Z.-T. Li, Y.-J. Lin, J.A. Thomson, L.-S. Turng, Fabrication and modification of wavy multicomponent vascular grafts with biomimetic mechanical properties, antithrombogenicity, and enhanced endothelial cell affinity, J. Biomed. Mater. Res. Part B Appl. Biomater. 107 (2019) 2397–2408. https://doi.org/10.1002/jbm.b.34333.

[62] W. Wang, D. Liu, D. Li, H. Hu, J. Zhang, Z. You, M. Li, C. He, Nanofibrous vascular scaffold prepared from miscible polymer blend with heparin/stromal cell-derived factor-1 alpha for enhancing anticoagulation and endothelialization, Colloids Surf. B Biointerfaces 181 (2019) 963–972. https://doi.org/10.1016/j.colsurfb.2019.06.065.

[63] A. Gao, R. Hang, W. Li, W. Zhang, P. Li, G. Wang, L. Bai, X.F. Yu, H. Wang, L. Tong, P.K. Chu, Linker-free covalent immobilization of heparin, SDF-1α, and CD47 on PTFE surface for antithrombogenicity, endothelialization and anti-inflammation, Biomaterials 140 (2017) 201–211. https://doi.org/10.1016/j.biomaterials.2017.06.023.

[64] P. Chiodelli, S. Rezzola, C. Urbinati, F. Federici Signori, E. Monti, R. Ronca, M. Presta, M. Rusnati, Contribution of vascular endothelial growth factor receptor-2 sialylation to the process of angiogenesis, Oncogene 36 (2017) 6531–6541. https://doi.org/10.1038/onc.2017.243.

[65] T. Nightingale, D. Cutler, The secretion of von Willebrand factor from endothelial cells; an increasingly complicated story, J. Thromb. Haemost. 11 (2013) Suppl 1 192–201. https://doi.org/10.1111/jth.12225.

[66] H. Yu, Y. Shen, J. Jin, Y. Zhang, T. Feng, X. Liu, Fluid shear stress regulates HepG2 cell migration though time-dependent integrin signaling cascade, Cell Adhes. Migr. 12 (2018) 56–68. https://doi.org/10.1080/19336918.2017.1319042.

[67] K. Lekesiz, B. Naumnik, H. Borysewicz-Sanczyk, E. Koc-Zurawska, M. Mysliwiec, Effect of unfractionated heparin, enoxaparin and sulodexide on the relations between secretion and expression of OPG, RANKL and vWF in HUVEC, Folia Histochem. Cytobiol. 51 (2013) 156–163. https://doi.org/10.5603/FHC.2013.0016.

[68] R.A. Hoshi, R. Van Lith, M.C. Jen, J.B. Allen, K.A. Lapidos, G. Ameer, The blood and vascular cell compatibility of heparin-modified ePTFE vascular grafts, Biomaterials 34 (2013) 30–41. https://doi.org/10.1016/j.biomaterials.2012.09.046.

[69] X.C. Liu, J. Zhao, Y. Wang, T.J. Liu, F. Lü, G.W. He, Heparin- and basic fibroblast growth factor-incorporated stent: a new promising method for myocardial revascularization, J. Surg. Res. 164 (2010) 204–213. https://doi.org/10.1016/j.jss.2009.05.005.

[70] P.J. Lenting, O.D. Christophe, C.V. Denis, von Willebrand factor biosynthesis, secretion, and clearance: connecting the far ends, Blood 125 (2015) 2019–2028. https://doi.org/10.1182/blood-2014-06-528406.

[71] C. Urbich, E. Dernbach, A. Reissner, M. Vasa, A.M. Zeiher, S. Dimmeler, Shear stress-induced endothelial cell migration involves integrin signaling via the fibronectin receptor subunits alpha(5) and beta(1), Arterioscler. Thromb. Vasc. Biol. 22 (2002) 69–75. https://doi.org/10.1161/hq0102.101518.

Table 1. Primer sequences used for Real-Time PCR analysis.

Primer	**Sequence**
VEGR2	F: GGAACCTCACTATCCGCAGAGT
	R: CCAAGTTCGTCTTTTCCTGGGC
vWF	F: CCTTGAATCCCAGTGACCCTGA
	R: GGTTCCGAGATGTCCTCCACAT
Integrin-α5 subunit	F: GCCGATTCACATCGCTCTCAAC
	R: GTCTTCTCCACAGTCCAGCAAG
RPL32	F: ACAAAGCACATGCTGCCCAGTG
	R: GCTCGCAGTACGACTACACTGAC

Journal Pre-proof

Table 2. Stress-strain areas recorded for control and functionalized SDVG scaffolds under dynamic loading cycles, and differences in areas recorded between the 2nd and the 20th peaks. Rings (3 mm height) were loaded at a constant rate of 0.17 mm/s to forces of 0.080 and 0.016 N, and at a constant rate of 0.33 mm/s to a force of 0.028 N. Mean values and, in parenthesis, standard deviation (n=3 for three independent measurements).

Scaffold	**Force (N)**	**Area$_{Peak2}$ (N·mm)**	**Area$_{Peak20}$ (N·mm)**	**ΔArea (%)**
Control	0.080	0.010 (0.001)	0.008 (0.001)	14.9 (14.1)
	0.016	0.020 (0.004)	0.019 (0.004)	5.0 (3.3)
	0.028	0.064 (0.004)	0.059 (0.004)	7.5 (0.1)
Functionalized	0.080	0.019 (0.004)	0.019 (0.004)	0.1 (1.0)
	0.016	0.043 (0.006)	0.042 (0.005)	1.4 (1.2)
	0.028	0.077 (0.020)	0.076 (0.020)	1.0 (0.8)

Journal Pre-proof

Figure Captions:

Figure 1. Optical images (first column) and SEM micrographs of control and heparin-immobilized SDVG. SEM micrographs of both inner and outer surfaces are shown at 1,000X (scale bar 10 μm) and 10,000X (scale bar 2 μm).

Figure 2. Engineering stress versus engineering strain plots recorded along longitudinal and transversal axes for control and heparin-functionalized SDVG, and recorded for ring sections of control and heparin-functionalized SDVG before and after 20 cycles of dynamic loading at 0.280 N.

Figure 3. Stress-strain behavior of control SDVG and heparin-functionalized SDVG recorded under dynamic loading cycles at forces of 0.080 N (A1, A2, B1, B2), 0.160 N (A3, A4, B3, B4) or 0.280 N (A5, A6, B5, B6). Peaks corresponding to the 1st, 2nd, and 20th cycle are shown in detail in even plots.

Figure 4. Confocal micrographs of representative fields of A) pristine SDVG and B) heparin-functionalized SDVG at 10X magnification. Adhered HUVECs were stained with phalloidin-Alexa fluor 488 (green; cytoplasm) and DAPI (blue; nucleus). Scale bars: 100 μm.

Figure 5. Relative surface area occupied by HUVECs grown on heparin-functionalized SDVG with respect to pristine SDVG (control).

Figure 6. Relative gene expression of HUVECs cultured on the surface of control and heparin-functionalized SDVG after seven days in culture under laminar flow.

Journal Pre-proof

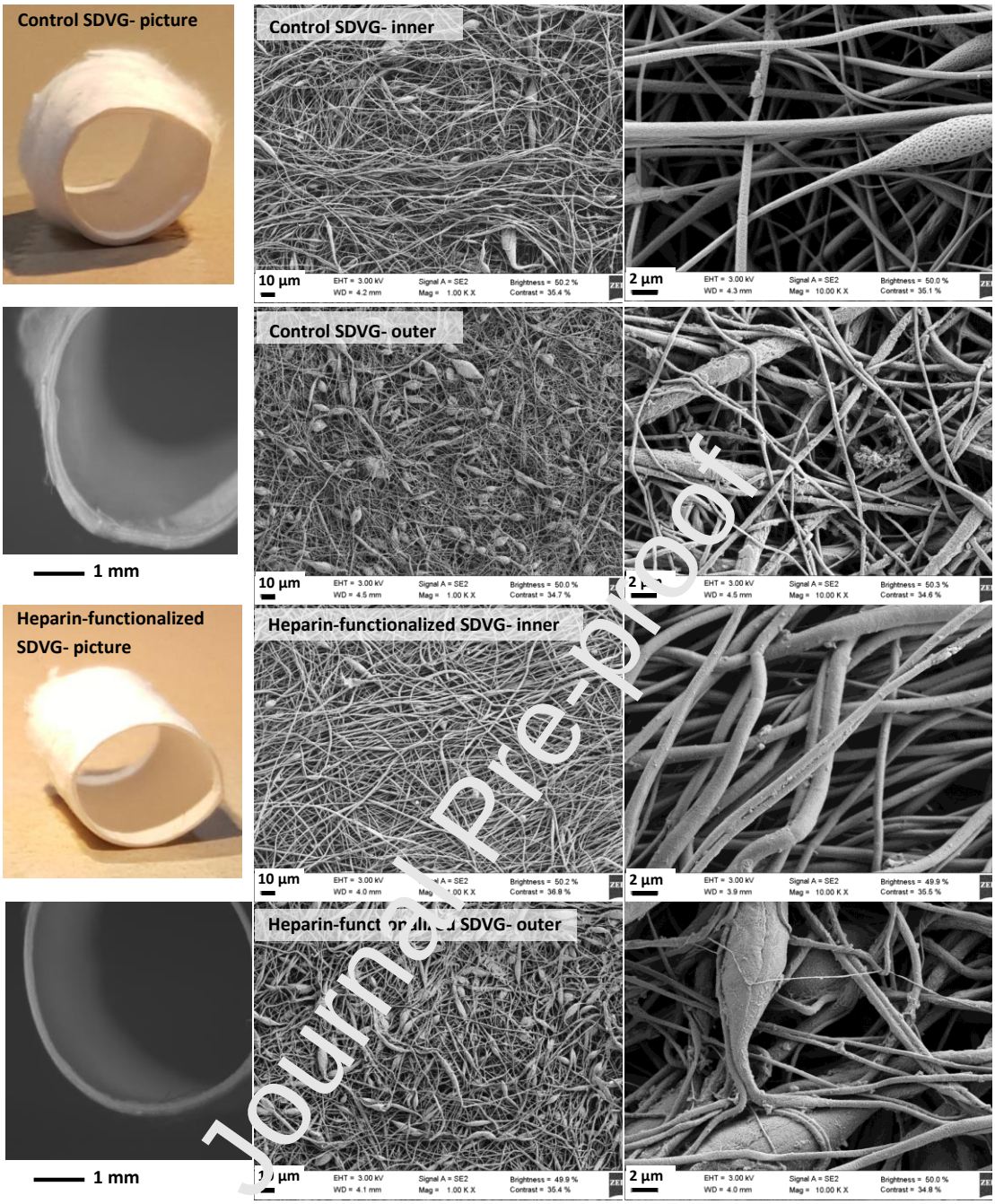

FIGURE 1

Journal Pre-proof

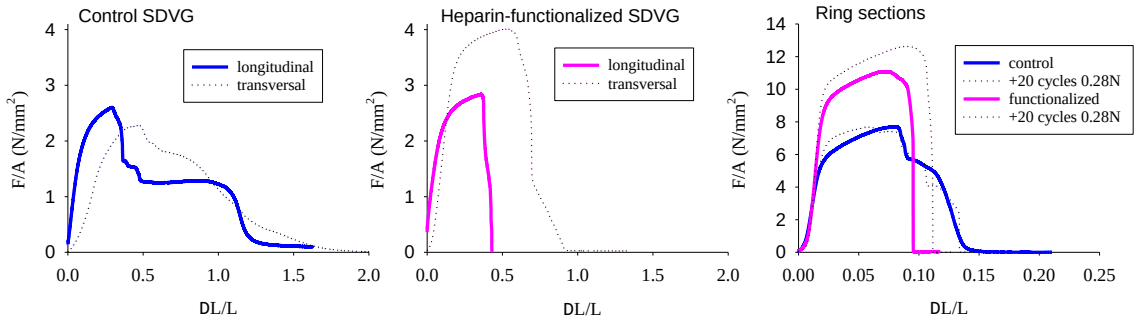

FIGURE 2

Journal Pre-proof

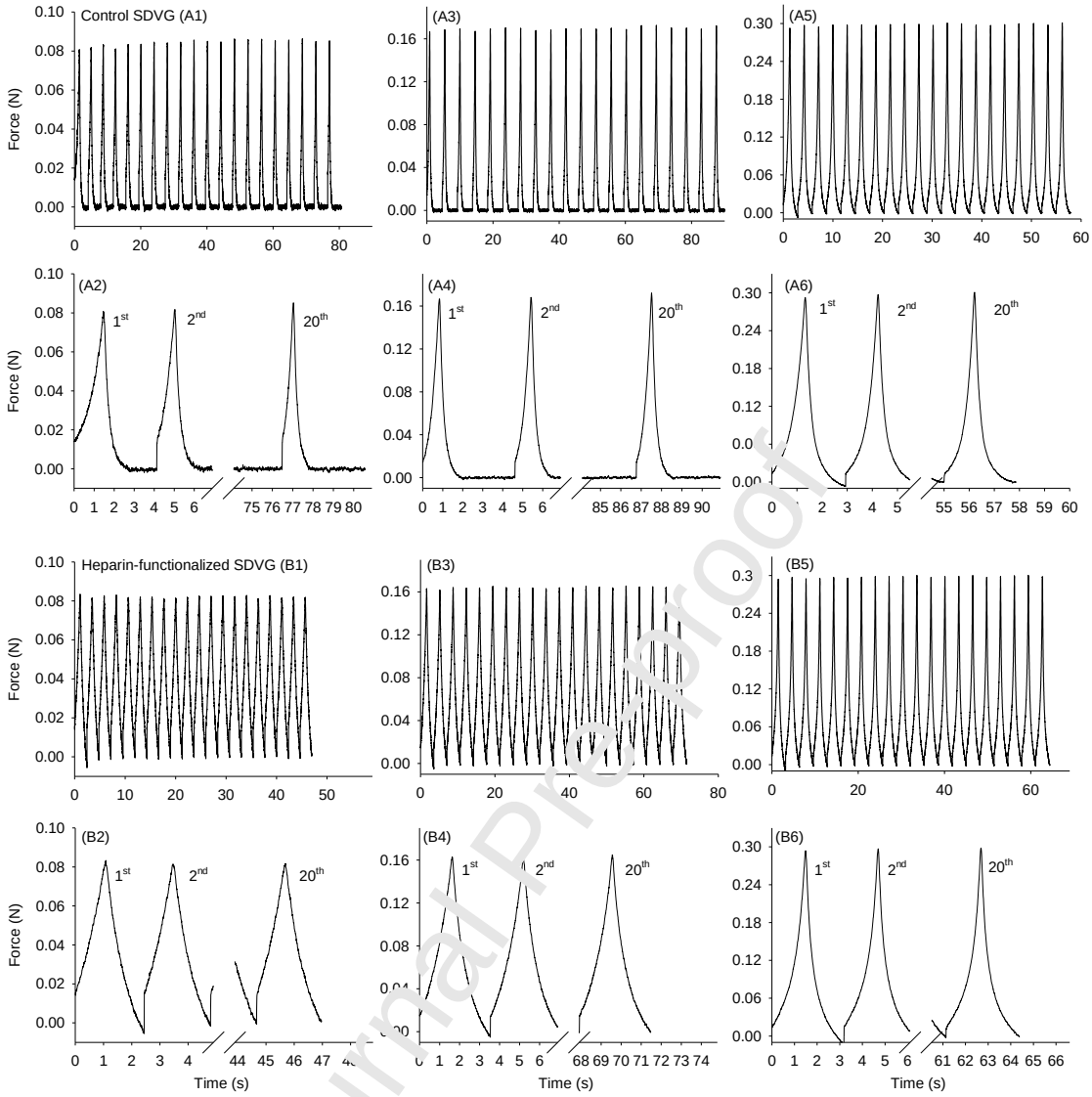

FIGURE 3

Journal Pre-proof

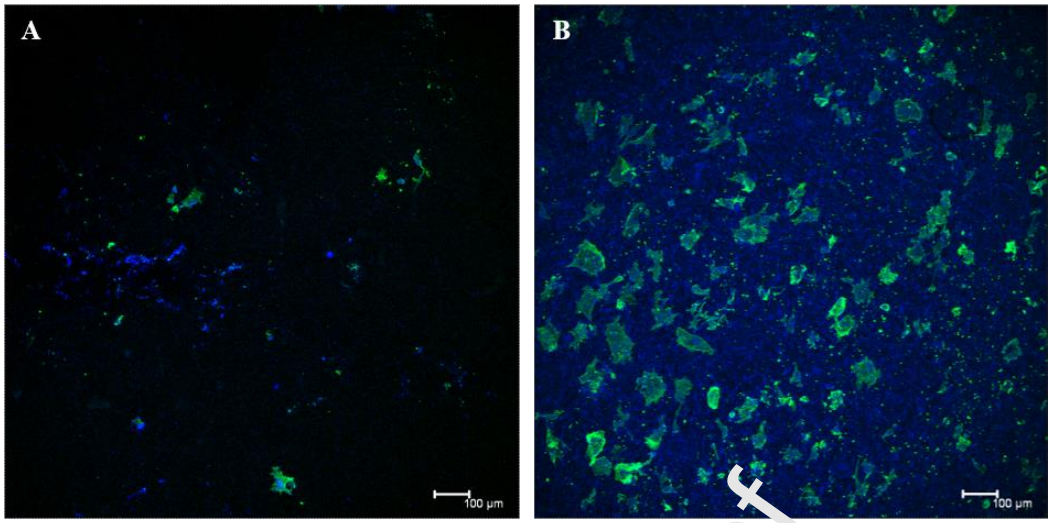

FIGURE 4

Journal Pre-proof

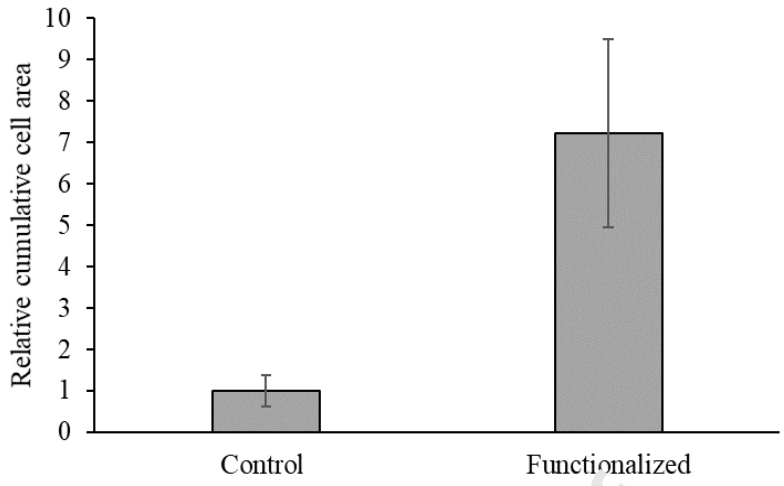

FIGURE 5

Journal Pre-proof

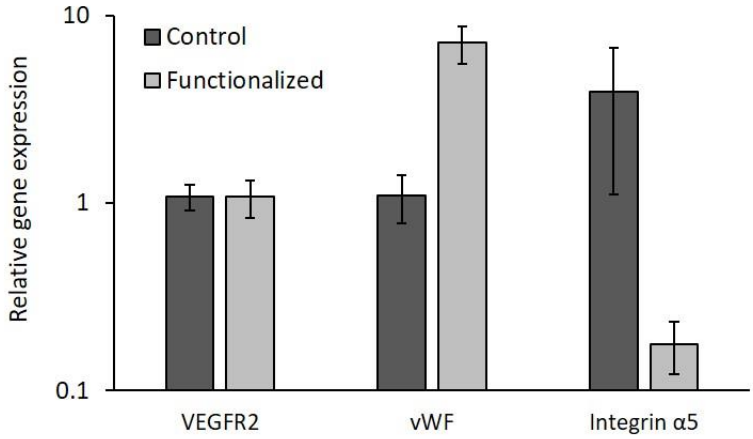

FIGURE 6

Journal Pre-proof

Declaration of competing interest

The authors declare that they have no known competing financial interests or personal relationships that could have appeared to influence the work reported in this paper.

Journal Pre-proof